Intimate genetic relationships and fungicide resistance in multiple strains of human pathogenic fungus *Aspergillus fumigatus* isolated from a plant bulb

Hiroki Takahashi[1,2,3], Sayoko Oiki[4], Yoko Kusuya[1], Syun-ichi Urayama[4,5], Daisuke Hagiwara[4,5,*]

[1] Medical Mycology Research Center, Chiba University, 1-8-1 Inohana, Chuo-ku, Chiba 260-8673, Japan

[2] Molecular Chirality Research Center, Chiba University, 1-33 Yayoi-cho, Inage-ku, Chiba 263-8522, Japan

[3] Plant Molecular Science Center, Chiba University, 1-8-1 Inohana, Chuo-ku, Chiba 260-8675, Japan

[4] Faculty of Life and Environmental Sciences, University of Tsukuba, 1-1-1 Tennodai, Tsukuba, Ibaraki 305-8577, Japan

[5] Microbiology Research Center for Sustainability, University of Tsukuba, 1-1-1 Tennodai, Tsukuba, Ibaraki 305-8577, Japan

* Corresponding author: D. Hagiwara

hagiwara.daisuke.gb@u.tsukuba.ac.jp

Running title

Plant bulb-derived azole resistant *A. fumigatus*

ORCIDs

D. Hagiwara: 0000-0003-1382-3914

H. Takahashi: 0000-0001-5627-1035

Summary

Fungal infections are increasingly dangerous because of environmentally-dispersed resistance to antifungal drugs. Azoles are commonly used antifungal drugs, but they are also used as fungicides in agriculture, which may enable enrichment of azole-resistant strains of the human pathogen *Aspergillus fumigatus* in the environment. Understanding of environmental dissemination and enrichment of genetic variation associated with azole resistance in *A. fumigatus* is required to suppress resistant strains. Here, we focused on eight strains of azole-resistant *A. fumigatus* isolated from a single tulip bulb for sale in Japan. This set includes strains with TR_{34}/L98H/T289A/I364V/G448S and TR_{46}/Y121F/T289A/S363P/I364V/G448S mutations in the *cyp51A* gene, which showed higher tolerance to several azoles than strains harboring TR_{46}/Y121F/T289A mutation. The strains were typed by microsatellite typing, single nucleotide polymorphism profiles, and mitochondrial and nuclear genome analyses. The strains grouped differently using each typing method, suggesting historical genetic recombination among the strains. Our data also revealed that some strains isolated from the tulip bulb showed tolerance to other classes of fungicide, such as QoI and carbendazim, followed by related amino acid alterations in the target proteins. Considering spatial-temporal factors, plant bulbs are an excellent environmental niche for fungal strains to encounter partners, and to obtain and spread resistance-associated mutations.

Introduction

Azoles are versatile compounds that show outstanding activity against a wide range of fungi, including plant and human pathogens. These compounds play an essential role in agricultural and clinical settings as fungicides and antifungal drugs (Fisher et al, 2018, Price et al, 2015). Their main mode of action is inhibition of the ergosterol biosynthesis pathway by inhibiting Cyp51, which functions as an 14-alpha-demethylase critical for the biosynthesis. Azole fungicides, known as demethylase inhibitors (DMIs), include triazole and imidazole compounds such as tebuconazole, propiconazole, triflumizole, and prochloraz. They are widely used to protect crops and fruits against pathogens by application during cultivation and postharvest preservation, as well as for seed disinfection. In medicine, azole drugs are essential options to combat dermatophytes and deep-seated fungal pathogens, such as *Trichophyton rubrum* and *Aspergillus fumigatus*, respectively. Azoles are the only class of compound used to control fungi in both agriculture and medicine.

A. fumigatus is a major causative agent of aspergillosis and ubiquitously present in the environment as a saprobe. A limited number of antifungals are approved for therapy of *A. fumigatus* infection; voriconazole (VRCZ) and itraconazole (ITCZ) are the first-line drugs for the treatment of pulmonary infection (Jenks and Hoenigl, 2018). However, this antifungal therapy is threatened by azole-resistant *A. fumigatus*, strains of which have been increasingly isolated since the beginning of this century (Howard et al, 2009). The resistance mechanisms to azole drugs that have been identified in *A. fumigatus* from clinical settings are mutations in Cyp51A, HMG-CoA reductase HMG1, and a subunit of CCAAT-binding complex HapE, and overexpression of *cdr1B*, which encodes an ABC transporter (Hagiwara et al, 2016a, Nywening et al, 2020, Hagiwara et al, 2018, Rybak et al, 2019, Camps et al, 2012, Hortschansky, et al, 2020, Fraczek et al, 2013). These azole resistance

mutations are thought to have emerged during therapy with prolonged azole treatment.

However, in addition to treatment-based resistance, environmentally derived resistance has been considered as a non-negligible source of azole drug resistance of *A. fumigatus* during the last decade (Berger et al, 2017, Lestrade et al, 2019). Typical resistant strains from the environment carry a tandem repeat (TR) and single-nucleotide polymorphisms (SNPs) in the promoter and coding regions of the *cyp51A* gene, respectively. The most prevalent variants are TR_{34}/L98H and TR_{46}/Y121F/T289A, which were isolated for the first time from patients in Europe in 1998 and North America in 2008, respectively (Jeanvoine et al, 2020). The mutants with TR_{34} typically show high resistance to ITCZ, whereas the strains with TR_{46} show VRCZ resistance, but some are pan-azole-resistant strains. These genotypes were later recovered from environments worldwide (Schoustra et al, 2019, Resendiz et al, 2018, Hagiwara, 2018). Diverse resistant mutants with tandem repeats in the Cyp51A-encoding gene have been reported (Table 1).

Table 1. Reported Cyp51A variants with tandem repeats in azole-resistant *A. fumigatus*

Cyp51A allele	Country	References
TR_{34}/L98H	Many places	-
TR_{46}/Y121F/T289A	Many places	-
TR_{53}	Colombia	Alvarez-Moreno et al, 2017
TR_{34}/L98H/S302N	The Netherlands	Schoustra et al, 2019
TR_{34}/L98H/F495I	The Netherlands	Schoustra et al, 2019
TR_{34}/L98H/L343H	The Netherlands	Schoustra et al, 2019
TR_{34}/L98H/E356V	The Netherlands	Schoustra et al, 2019
TR_{34}/L98H/S297T/F495I	The Netherlands	Schoustra et al, 2019, Cao et al, 2020

TR_{34}/L98H/T289A/I364V/G448S	Japan	Nakano et al, 2020, this study
TR_{46}/Y121F/T289A/I364V	The Netherlands	Schoustra et al, 2019
TR_{46}/Y121F/M172I/T289A/G448S	The Netherlands, Japan, Iran	Zhang et al, 2017, Nakano et al, 2020, Ahangatkani et al, 2020, Fraaije et al, 2020
TR_{46}/Y121F/T289A/S363P/I364V/G448S	The Netherlands, Japan	Nakano et al, 2020, Fraaije et al, 2020, Zhang et al, 2021, this study
TR^{3}_{46}/Y121F/M172I/T289A/G448S	The Netherlands, Japan	Zhang et al, 2017, Nakano et al, 2020
TR^{4}_{46}/Y121F/M172I/T289A/G448S	The Netherlands	Zhang et al, 2021
TR_{92}/Y121F/M172I/T289A/G448S	The Netherlands	Zhang et al, 2021

Recently, a possible environmental hot spot for azole-resistant *A. fumigatus* was proposed (Zhang et al, 2017). The TR-type mutants were prevalently isolated from agricultural compost containing azole fungicide residues, whereas azole-free compost was dominated by wild-type (WT) *A. fumigatus*. This view was also supported in other studies (Schoustra et al, 2019, Zhang et al, 2021), indicating that azole-resistant strains are enriched under the selective pressure of environmental azoles. The work by Zhang *et al*. also suggested that sexual reproduction plays an important role in developing and evolving new *cyp51A* alleles for drug resistance in compost (Zhang et al, 2017). Taking into consideration that TR-type drug-resistant *A. fumigatus* mutants show cross-resistance to DMIs (Snelders et al., 2012), azole-containing environmental niches may serve as evolutionary incubators through genetic recombination.

The propagation of azole-resistant *A. fumigatus* has been studied in an epidemiological manner using microsatellite analysis by short tandem repeats for *A. fumigatus* (STR*Af*), which is a widely accepted intraspecies typing method with high-resolution discriminatory power (de Valk et al, 2005). TR-type mutant strains were spread worldwide. Some isolates from multiple countries were genetically closely related to each other and some had identical microsatellite

patterns (Pontes et al, 2020, Cao et al, 2020, Wang et al, 2018, Hagiwara et al, 2016b). Besides such international propagation, intranational clonal expansion was also reported in several countries (Ahangarkani et al, 2020, Chowdhary et al, 2012). Recent population genomic studies revealed that the azole-resistant strains are globally distributed. The isolates were divided into two broad clades, and TR mutants belong to the populations in an uneven manner (Sewell et al, 2019). These data suggest that azole resistance primarily expanded by asexual and sexual propagation from a limited number of ancestors with TR-type mutation, rather than locally and independently emerging in each environment.

It was recently proposed that resistant *A. fumigatus* strains are transferred internationally via imported plant bulbs (Dunne et al, 2017). Plant bulbs produced in the Netherlands and sold in Ireland were contaminated with TR-type *A. fumigatus* mutants. Similar cases were also reported by two independent Japanese groups (Hagiwara 2020, Nakano et al, 2020); azole-resistant *A. fumigatus* with diverse Cyp51A variants were isolated from plant bulbs that were imported from the Netherlands and sold in Japanese gardening shops. These studies suggest that the wide spread of azole-resistant *A. fumigatus* mutants is attributable in part to trade in agricultural products including plant bulbs.

In the present study, to further understand genetic variations in plant bulb-associated isolates, we focused on eight *A. fumigatus* strains that were co-isolated from a single tulip bulb in a previous screening study (Hagiwara, 2020). Sensitivity to medical and agricultural azoles, as well as other classes of fungicides, was compared between the strains. Whole genome comparison of the eight strains showed several fragmental overlaps of their genomes, suggesting genetic recombination had occurred between strains in the single bulb. Our work indicates that plant bulbs are not only a vehicle for the pathogen but also a place where the pathogen can evolve its drug resistance.

Results

Variation of Cyp51A mutation in strains from a single bulb

In a previous study, eight strains of *A. fumigatus* were isolated from a single tulip bulb as different colonies (hereafter referred to as strains 3-1-A to 3-1-H) (Hagiwara, 2020). Strain 3-1-H has no TR or SNPs in *cyp51A*, whereas TR_{34} or TR_{46} occur in combination with various SNPs in the other seven strains (Table 2). Strains 3-1-A, 3-1-E, 3-1-F, and 3-1-G have a typical variant, TR_{46}/Y121F/T289A. Strain 3-1-D has mutations S363P, I364V, and G448S as well as TR_{46}/Y121F/T289A. Strains 3-1-B and 3-1-C have TR_{34}/L98H and mutations T289A, I364V, and G448S. Notably, TR_{34}/L98H and G448S are known to play a role in azole resistance, and T289A is typically accompanied by TR_{46} (Hagiwara et al, 2016a). Thus, the Cyp51A of strains 3-1-B and 3-1-C showed complicated sequence variation, including three mutations related to azole resistance.

Table 2. Cyp51A variation and microsatellite typing of the strains in this study

Strain ID	Cyp51A variation	2A	2B	2C	3A	3B	3C	4A	4B	4C
3-1-A	TR_{46}/Y121F, T289A	10	20	8	44	9	10	8	10	7
3-1-B	TR_{34}/L98H, T289A, I364V, G448S	23	10	9	35	9	6	8	10	18
3-1-C	TR_{34}/L98H, T289A, I364V, G448S	23	10	9	35	9	6	8	10	18
3-1-D	TR_{46}/Y121F, T289A, S363P, I364V, G448S	24	20	12	45	9	11	8	10	18
3-1-E	TR_{46}/Y121F, T289A	26	20	12	36	9	22	8	14	31
3-1-F	TR_{46}/Y121F, T289A	25	20	12	45	11	6	10	12	18
3-1-G	TR_{46}/Y121F, T289A	23	10	9	36	9	6	12	10	7
3-1-H	wt	23	19	15	33	11	7	13	9	5

Varied sensitivity to azoles in the strains from a single bulb

As previously reported, strains 3-1-A to G, which have TRs in *cyp51A*, showed VRCZ resistance (>32 µg/ml) in minimum inhibitory concentration tests (Hagiwara, 2020). To further understand the susceptibility to azole drugs, colony growth was evaluated on potato-dextrose-agar (PDA) containing 10 µg/ml of VRCZ (Fig. 1A). Strains 3-1-B, 3-1-C, and 3-1-D were more tolerant to VRCZ than the other strains. When grown on medium containing DMIs (triflumizole, imazalil, prochloraz, tebuconazole, epoxiconazole, or difenoconazole), strain 3-1-H, which harbors WT Cyp51A, showed the greatest growth inhibition among the strains. Strains 3-1-B, 3-1-C, and 3-1-D were less affected by the DMIs (except prochloraz) (Fig. 1B). On the basis of colony diameter measurement, strains 3-1-B, 3-1-C and 3-1-D showed higher tolerance to VRCZ and DMIs than strains 3-1-A, 3-1-E, 3-1-F, and 3-1-G (Fig. 1C). These results suggest that the combination of TR and G448S mutation increases resistance to azole compounds.

The expression levels of genes related to azole resistance were examined in the eight strains by quantitative real-time (qRT)-PCR. Compared with strain 3-1-H, which has the WT *cyp51A* gene, strains with a TR in the *cyp51A* gene showed higher expression of *cyp51A* (Fig. 2A). Overexpression of *cdr1B*, which encodes an ABC transporter, has been reported to confer azole resistance. Thus, the expression level of *cdr1B* was also determined in the eight strains by qRT-PCR. Strains 3-1-B and 3-1-C showed relatively high expression levels of *cdr1B* (Fig. 2B).

Microsatellite typing analysis of tulip bulb isolates

To investigate the genetic relationships between the eight strains co-isolated from a single tulip bulb, microsatellite analysis using STR*Af* was performed (Table 2). This analysis also included TR-type strains that were previously reported and isolated in different countries and strains isolated from plant bulbs

in Japan (Nakano et al, 2020, Hagiwara, 2020) (Fig. 3). Among the eight strains, the STR*Af* patterns of 3-1-B and 3-1-C matched perfectly. Strain 3-1-D is closely related to them, as this strain contains the same number of STRs in 4 of the 9 panels. Similarly, strain 3-1-D shares the same number of STRs as strain 3-1-F in 4 of the 9 panels. These four strains grouped into the same clade. The other strains were distantly positioned in the dendrogram. Interestingly, some strains that were isolated from plant bulbs in the study by Nakano *et al*. (2020) showed a close relationship with our strains. NGS-ER15 had an STR pattern similar to that of our strains 3-1-B and 3-1-C (5 of the 9 panells), which is consistent with these strains having the same Cyp51A allele (TR_{34}/L98H/T289A/I364V/G448S). Strains NGS-ER6 and NGS-ER7 of Nakano *et al*. (2020) are closely related to strains 3-3-A and 3-3-B that were isolated from a single another tulip bulb in our previous study (Hagiwara, 2020). Note that these extraordinarily close relatives were isolated from plant bulbs in different laboratories.

Genome sequencing and comparison between strains

To gain more insight into genetic differences or relatedness, genomes of the eight strains (3-1-A to H) were sequenced using the Illumina platform. Complete mitochondrial genomes were successfully obtained for the strains (31,749 to 31,770 base pairs [bp] long) (Table 3). A phylogenetic tree was constructed using the mitochondrial genomes and those of other strains (IFM 61407, IFM 59365, and IFM 61578) that had been clinically isolated in Japan (Takahashi-Nakaguchi et al, 2015) (Fig. 4A). This dendrogram indicated that the eight strains isolated from the tulip bulb can be divided into three groups. Group m1 contains strains 3-1-A, 3-1-D, and 3-1-G; strains 3-1-B, 3-1-C, 3-1-E, and 3-1-F are in Group m2. Strain 3-1-H was distantly positioned from both Group m1 and m2. Differences in the length of the mitochondrial genome well reflect the grouping, suggesting that strains within each group are very close relatives.

Table 3. Results of genome sequencing for strains isolated from a single tulip bulb

Strain ID	Total length of chromosomes [bp]	GC [%]	# of proteins	Mitochondrial genome [bp]	Mito Group	CSP type	Mating type
3-1-A	28,889,155	49.342	9,492	31,770	m1	t02	*mat1-1*
3-1-B	28,519,682	49.352	9,359	31,763	m2	t02	*mat1-1*
3-1-C	28,533,261	49.355	9,490	31,763	m2	t02	*mat1-1*
3-1-D	29,087,830	49.324	9,515	31,770	m1	t02	*mat1-1*
3-1-E	28,703,796	49.398	9,464	31,763	m2	t02	*mat1-1*
3-1-F	28,808,510	49.492	9,537	31,763	m2	t02	*mat1-2*

In the microsatellite typing analysis described above, strains 3-1-B, 3-1-C, 3-1-D, and 3-1-F were grouped into the same clade, but this was inconsistent with the grouping based on mitochondrial genomes, in which strain 3-1-D was not in the same group as strains 3-1-B, 3-1-C, and 3-1-F.

3-1-G	29,178,518	49.295	9,543	31,770	m1	t02	*mat1-1*
3-1-H	28,716,638	49.611	9,617	31,749	m3	t01	*mat1-1*

Nuclear genomes of the eight strains were compared with the reference genome of *A. fumigatus* strain Af293 (retrieved from AspGD, http://www.aspgd.org/) ; 92.2% to 93.6% of the Af293 genome was covered in the eight strains, and 69,949 to 79,391 SNPs were detected the genomes of the eight strains compared with the sequence of Af293 (Table 4). Phylogenetic analysis of the eight strains and previously-sequenced strains was performed by using concatenated sequences of the SNP positions (Takahashi-Nakaguchi et al, 2015) (Fig. 4B). Among the eight strains, 3-1-H was distantly positioned in the dendrogram as an independent clone. The other seven strains showed moderately close genetic-relatedness to each other based on comparison with the apparently independent clinical strains. Strains 3-1-B and 3-1-C showed the closest relationship, which was supported by the lowest number (6,241) of SNPs between strains (Table 4). This is consistent with the results of microsatellite and mitochondrial genome typing. Nevertheless, in the mitochondrial genome typing, strain 3-1-E was in Group m2 with strains 3-1-B, 3-1-C, and 3-1-F; however, strain 3-1-E was relatively distant from these three strains in phylogenetic analysis based on the nuclear genome (Fig. 4C).

From the genome sequences, CSP typing was performed, which can typify strains by sequence variation at a single locus (*csp*: Afu3g08990) (Klaassen et al, 2009). The results showed that seven strains (3-1-A to 3-1-G) carried an identical type (t02), but strain 3-1-H strain had type t01. Sequence analysis for mating type revealed that all but strain 3-1-F harbored *mat1-1*, whereas 3-1-F carried *mat1-2* (Table 3).

Comparison of genome-wide SNP frequency pattern

Inconsistency in strain typing among the typing methods using the mitochondrial and chromosomal genome sequences caused us to speculate that genetic recombination had occurred between the strains isolated from the single tulip bulb. To help test this hypothesis, the SNP frequency and distribution were investigated and compared among the strains in a genome-wide manner (Fig. S1). There were several regions where the patterns of SNP frequency markedly differed among the strains (Fig.

Table 4. Summary of SNPs in strains isolated from a single tulip bulb.

Strain ID	% of covered positions *1	# of SNPs *1	3-1-A	3-1-B	3-1-C	3-1-D	3-1-E	3-1-F	3-1-G	3-1-H
3-1-A	92.7%	74,865								
3-1-B	92.2%	77,715	46,380							
3-1-C	92.2%	77,879	46,296	6,241						
3-1-D	93.3%	78,394	38,184	46,181	46,244					
3-1-E	92.6%	76,218	50,656	56,072	55,902	59,081				
3-1-F	93.0%	75,553	40,062	45,535	45,284	52,533	54,507			
3-1-G	93.0%	79,391	32,777	36,509	36,566	36,517	57,646	44,451		
3-1-H	93.6%	69,949	95,960	91,751	91,720	88,448	89,321	92,982	93,204	

*1 These are relative to the genome of reference strain *A. fumigatus* Af293.

Table 5. The number of orthologous genes in the strains isolated from a single tulip bulb compared with reference strain *A. fumigatus* Af293.

Chromosome		# of orthologous genes compared with strain Af293

	Af293	3-1-A	3-1-B	3-1-C	3-1-D	3-1-E	3-1-F	3-1-G	3-1-H
chr1	1,642	1,369	1,355	1,377	1,371	1,369	1,365	1,370	1,370
chr2	1,640	1,433	1,406	1,425	1,425	1,411	1,436	1,427	1,433
chr3	1,395	1,163	1,163	1,169	1,179	1,152	1,173	1,179	1,189
chr4	1,253	1,089	1,075	1,093	1,090	1,098	1,096	1,085	1,095
chr5	1,367	1,151	1,156	1,160	1,153	1,153	1,162	1,156	1,153
chr6	1,249	1,068	1,067	1,074	1,058	1,069	1,073	1,070	1,080
chr7	651	490	478	476	483	489	493	494	489
chr8	628	502	496	507	497	505	506	491	513
Total	9,825	8,265	8,196	8,281	8,256	8,246	8,304	8,272	8,322

S1). For example, regions 5-A, 5-B, and 5-C on chromosome 5 were particularly characteristic (Fig. 5A). In region 5-A, strains 3-1-A, 3-1-E, and 3-1-H showed similar patterns of SNP frequency. In region 5-B, the pattern of strain 3-1-A was similar to that of strains 3-1-F and 3-1-H. In region 5-C, the pattern of strain 3-1-A was similar to that of strains 3-1-E, 3-1-G, and 3-1-H. These results indicate that strain 3-1-A shares parts of the sequence of chromosome 5 with strains 3-1-E, 3-1-F, 3-1-G, and 3-1-H. Such intergenomic variations were also found on other chromosomes (Fig. 5B, Fig. S1). These results showed a genome-wide mosaic pattern of SNP frequency, which is indicative of genetic recombination events in the strains.

Comparing genome-wide distribution of orthologous genes

To further investigate genome shuffling in the strains, we compared the patterns of orthologous among the strains isolated from the tulip bulb. First, the genes shared with the reference genome of *A. fumigatus* strain Af293 were investigated based on reciprocal blast hits (RBHs), which resulted in the isolates containing 8,196 to 8,322 orthologs of genes in strain Af293 (Table 5). The positions of the orthologs were generally evenly distributed in the strains,

although fewer orthologs were found on chromosome 7. Notably, different patterns of ortholog content were displayed in some regions of the genomes of the various strains (Fig. 6). I.e., some sets of strains have lost particular sets of genes, and other sets of genes have been lost in other sets of strains. Hence, the set of strains that shares an ortholog pattern is different at each locus (Fig. 6). This suggests repeated genome shuffling among the strains.

Varied tolerance to agricultural fungicides

As these strains were derived from a horticultural product, they may have been exposed to agricultural fungicides besides DMIs. Hence, the susceptibility of the eight strains to QoI (pyraclostrobin), SDHI (boscalid), methyl benzimidazole carbamate (carbendazim), and phenylpyrrole (fludioxonil) was evaluated on PDA plates. There was no significant difference among the strains in susceptibility to fludioxonil and boscalid (Fig. 7A&B). However, the colony of strain 3-1-H was smaller than those of the other seven strains on the medium containing pyraclostrobin or carbendazim. These results suggest that there is varied tolerance to pyraclostrobin and carbendazim among the strains.

From the genome sequences, mutations that are possibly responsible for tolerance to carbendazim and pyraclostrobin were searched in the target molecules tubulin and cytochrome b that are encoded by *tubA* (Afu1g10910) and *cytB* (AfuMt00001), respectively (Fig. 6C). The amino acid substitution F219Y was found in TubA of strains 3-1-A to 3-1-G. This substitution has been reported in several carbendazim-resistant strains of plant pathogenic fungi (Yarden and Katan, 1993, Zhou et al, 2020). To investigate how the mutation is distributed in human pathogenic *A. fumigatus* genomes, the SNP database in FungiDB was explored. According to the dataset, 18% (14 of 77 strains) of *A. fumigatus* contain F219Y in TubA. Notably, eight of the 77 strains were isolated from the environment, and four of these possess the amino acid substitution.

In CytB, mutations V13I and G143A were found in strains 3-1-A to 3-1-G, and V119I was found in 3-1-H. G143A in CytB has been reported to confer the resistance to QoI in many plant pathogenic fungi (Samuel et al, 2011, Bolton et al, 2012), suggesting that this mutation in *A. fumigatus* is related to low sensitivity to QoI fungicide. As mitochondrial genome sequences are scarce in public databases, we investigated the sequence of the *cytb* gene in nine strains that were clinically isolated in a previous study and whose mitochondrial genome sequence is at least partly available (Takahashi-Nakaguchi et al, 2015). Among these nine strains, no G143A mutation was observed, whereas seven of the strains contain V119I (as also observed in our strain 3-1-H).

Discussion

The distribution of azole-resistant *A. fumigatus* in natural environments has drawn increasing attention in recent years, with special interest in where the resistant strains have emerged, inhabit, and have been translocated to. However, deep understanding is still lacking. In this work, to fill in gaps in knowledge, we focused on strains that were isolated from a single tulip bulb.

Sexual reproduction of *A. fumigatus* was demonstrated in laboratory conditions in 2009 (O'Gorman et al., 2009). After this discovery, researchers paid more attention to the pan-genome of clinical isolates of this pathogenic fungus. However, gene flow in the environment has been poorly studied. Population genetics study using linkage disequilibrium analysis for genetic markers supported the view that *A. fumigatus* reproduces asexually and sexually in natural habitats (Klaassen et al., 2012). However, although there is accumulating evidence for genetic recombination in nature, proving the occurrence of sexual reproduction is difficult unless one can directly collect cleistothecia and ascospores formed in the environment. Genetic recombination in sexual development is suggested to cause the emergence of TR mutation in

328 *cyp51A* gene through unequal crossover (Zhang et al., 2017). Thus, sexual
329 reproduction is considered both to spread mutations by fusion with other strains
330 and production of progeny, and to locally produce *de novo* TR mutations, which
331 could affect the prevalence of resistance to drugs and fungicides. Our data show
332 that seven of the eight isolates from a single tulip bulb contain TR mutations, and
333 the genetic variation between the TR-containing strains is low compared with
334 that between apparently independent strains. In addition, on the basis of
335 genome-wide distributions of SNPs and orthologous genes, genetic
336 recombination is likely to have occurred between the seven strains.
337 Co-isolation of the strains from a single bulb indicates that they have had
338 much opportunity to physically interact with each other inside or on the bulb. In
339 addition to the close spatial relationship of the fungal strains, they may interact
340 for a long time. In the conventional process of plant bulb production, bulbs are
341 multiplied from a parental bulb. This bulb multiplication is continued every year,
342 which presumably causes the sustained presence of the fungi on/inside the
343 bulbs. As described here, several strains were attached to a single bulb. These
344 strains might have encountered others and genetically mixed many times. Once
345 mutations giving rise to resistance to azoles emerged, the mutations could be
346 preferentially and stably retained in the microbial community inside the bulb.
347 Sequencing analysis of the eight strains produced complete mitochondrial
348 genomes and chromosomal genomes. The mitochondrial genome was of great
349 help in interpreting whether there had been sexual reproduction among the
350 strains. On the basis of mitochondrial genome sequences, the strains with TR
351 mutation can be classed into Groups m1 and m2 (Fig. 4A). The length and
352 sequences of the mitochondrial genomes are highly conserved in each group,
353 indicating that they are genetically close progenies. However, the chromosomal
354 genomes were diverse among the strains with TR mutation to the extent that
355 there were 32,000 to 59,000 SNPs, excepting strains 3-1-B and 3-1-C which had

356 approximately 6,200 SNPs (Table 4). The differences in grouping based on
357 mitochondrial and chromosomal genomes strongly suggested a genetic
358 recombination event. We therefore propose that the complete mitochondrial
359 genome is valuable for gaining deeper insight into genetic relatedness among
360 and between environmental and clinical isolates.
361 Strains with complicated *cyp51A* alleles have been reported in the literature
362 and this paper (Table 1). For instance, we have isolated *A. fumigatus* strains
363 with TR_{34}/L98H/T289A/I364V/G448S (3-1-B and 3-1-C) and
364 TR_{46}/Y121F/T289A/S363P/I364V/G448S (3-1-D) mutations in the *cyp51A* gene.
365 TR_{34}/L98H is a typical TR-type mutation conferring resistance to ITCZ and in
366 some cases to VRCZ, whereas TR_{46}/Y121F/T289A confers resistance to VRCZ
367 and in most cases to ITCZ (van Ingen et al, 2015, Buil et al, 2018). Amino acid
368 substitution G448S contributes to resistance to VRCZ and occasionally to ITCZ
369 (Bellete et al, 2010, Toyotome et al, 2016, Cao et al, 2020). Our finding that
370 three strains (3-1-B, 3-1-C, and 3-1-D) showed a higher tolerance to VRCZ and
371 some DMIs than strains with only TR_{46}/Y121F/T289A mutation is suggestive of
372 elevation of tolerance to azole drugs by combining mutations. Importantly,
373 strains with G448S mutation have been isolated not only from clinical samples
374 but also from soil (Cao et al, 2020). We cannot rule out the possibility that the
375 G448S mutation originally emerged and was retained in strains with
376 TR_{46}/Y121F/T289A under the selective pressure of fungicides.
377 The *A. fumigatus* strains used in the present work were isolated from a tulip
378 bulb by culturing at 45°C on plates containing medium supplemented with
379 fluconazole to select fungi that were resistant to fluconazole (Hagiwara 2020). In
380 total in that study, *A. fumigatus* was isolated from 50.8% of tulip bulbs (96/189),
381 and strains isolated from 20.6% of the bulbs (39/189) had TR mutation. Because
382 *A. fumigatus* is a saprophytic fungus that widely inhabits soil, compost, plant
383 debris, wood chips, the air, and aquatic environments, it was not surprising that

half of the tulip bulbs were contaminated with *A. fumigatus*. However, we have no idea how the fungus resides on or inside the bulbs from a biological viewpoint. Because of the high frequency of *A. fumigatus* isolation from tulip bulbs, there might be certain mechanisms by which *A. fumigatus* colonizes and infects the plant tissue, enabling persistence across bulb progenies. Notably, some *A. fumigatus* strains were isolated from *Citrus macrocarpa*, *Myricaria laxiflora*, *Ligusticum wallichii*, and *Moringa oleifera* (Francisco et al, 2020, Qin et al, 2019, Li et al, 2020, Arora and Kaur, 2019) as an endophyte. In general, however, the view that *A. fumigatus* has an endophytic mode in its life cycle remains to be established. In consideration of the dynamic mobilization of *A. fumigatus* in the environment, its association with plants may be overlooked, and we should pay more attention to it.

Recently, several field studies were published in which the prevalence of azole-resistant *A. fumigatus* was investigated in association with fungicide use. Work by Zhou *et al*. (2021) demonstrated that the concentration of triazoles in the soil of greenhouses was not significantly correlated with azole susceptibility of isolates. In another study from Germany, a low frequency of azole-resistant isolates from crop fields was reported regardless of azole fungicide use (Barber et al, 2020). A study by Frasije *et al*. (2020) also reported a low number of azole-resistant isolates in the soils of wheat-cropping fields subjected to fungicide treatment. The authors considered that arable crop production is low risk for development of azole resistance. Conversely, a large-scale survey across China was conducted, which showed that the residual level of azole fungicides in paddy soils positively correlated with the prevalence of azole-resistant *A. fumigatus* (Cao et al, 2021). Field research on azole-resistant *A. fumigatus* has started in many countries. More studies are required on the effects of fungicide use on the occurrence and spread of azole-resistant *A. fumigatus* in the environment, including agricultural and horticultural settings.

In plant bulbs, there may be other pathogenic and nonpathogenic fungi beside *A. fumigatus*. They are also exposed to fungicides when the bulbs are treated with fungicide. Repeated use of fungicides would facilitate the occurrence of resistance mutations in non-targeted fungi as well as in the target fungi of the pesticide. In the present study, we found that mutations in CytB and TubA that are related to resistance to QoI and carbendazim fungicides, respectively, were detected in *A. fumigatus* strains as an example of non-target fungi. These mutations might have been resulted from fungicide exposure during bulb production. Importantly, identical mutations of *A. fumigatus* were reported by Fraaije *et al*. (2020) and are found in database. These findings suggest that mutations related to resistance to antifungal agents are already present in the genomes of environmental fungi regardless of their pathogenicity. The boundary between acquired and natural resistance to antifungal compounds may become unclear in the near future.

Materials and Methods

Strains and culture conditions

Strains 3-1-A to 3-1-H used in this study were obtained in previous study and were isolated from a single tulip bulb (Hagiwara, 2020). For plate and liquid cultures, PDA and potato-dextrose broth (PDB) were used, respectively. For colony growth tests, 10^5 conidia of each strain were inoculated and incubated for 48 h at 37°C before taking pictures. Insusceptibility tests, 10 µg/ml VRCZ, imazalil, prochloraz, triflumizole, tebuconazole, epoxiconazole, and difenoconazole were respectively added to PDA. The control plate contained the equivalent volume of dimethylsulfoxide (DMSO). For measuring colony diameter, the culture time was 28 or 30 h. The data were obtained in triplicate, and the mean and standard deviation are presented. The fungicides fludioxonil,

carbendazim, boscalid, and pyraclostrobin were used at 0.2 µg/ml, 5 µg/ml, 2.5 µg/ml, and 10 µg/ml, respectively.

Quantitative real-time RT-PCR

Strains were cultured in PDB at 37°C for 18 h and harvested. The mycelia were frozen in liquid nitrogen, and total RNA was isolated using Sepasol Super G (Nacalai Tesque, Kyoto, Japan). cDNA was obtained by reverse transcription reaction using the total RNA sample and ReverTra Ace qPCR RT Master Mix with gDNA remover (TOYOBO, Osaka, Japan).

Real-time RT-PCR was performed using Brilliant III Ultra-Fast SYBR Green QPCR Master Mix (Agilent Technologies, Inc., Santa Clara, CA, USA) as described previously (Ninomiya et al, 2020). Relative expression ratios were calculated using the comparative cycle threshold (Ct) method. The actin-encoding gene was used as a normalization reference. Each sample was tested in triplicate, and the standard deviation is presented. The primer sets used were described in Hagiwara et al, 2017.

Microsatellite typing

Microsatellite typing was performed as described previously (Hagiwara et al, 2014). Briefly, nine microsatellite regions of approximately 400 bp were PCR amplified using purified genome DNA as a template and sequenced by the Sanger method. The repeat numbers of each locus were counted from the sequences. A dendrogram was constructed using Cluster 3.0 by hierarchical clustering with City-block distance for average linkage, and drawn using Treeview ver. 1.1.6r2 (de Hoon et al, 2004, Saldanha, 2004).

Genome sequencing

Whole-genome sequencing using next-generation methods was performed as described previously (Hagiwara et al., 2018). In brief, we extracted genomic DNA from overnight-cultured mycelia with NucleoSpin Plant II (Takara Bio, Shiga, Japan). For paired-end library preparation, an NEBNext Ultra DNA Library Prep Kit (New England BioLabs, MA, USA) and NEBNext Multiplex Oligos (New England BioLabs) were used in accordance with the manufacturer's instructions. A total of 11 strains including 3-1-A to 3-1-H, IFM 59365, IFM 61407, and IFM 61578 were sequenced. Paired-end sequencing (150-bp) on a HiSeq 4000 system (Illumina, San Diego, CA, USA) was carried out by GENEWIZ (South Plainfield, NJ, USA).

SNP detection

In addition to the abovementioned 11 strains, we used raw data for seven strains for comparison, which have been taken in a study by Takahashi-Nakaguchi et al (2015). Adapters and low-quality bases from Illumina reads were trimmed by fastp (ver. 0.20.1) (Chen et al., 2018). Filtered reads were aligned against the *A. fumigatus* strain Af293 reference genome using BWA (ver. 0.7.17-r1188) (Li and Durbin 2009). SNP detection was performed as described previously (Hagiwara et al., 2018). Briefly, SNPs were identified by using SAMtools (ver. 1.9) (Li et al., 2009) and filtered with >20-fold coverage, >30 mapping quality, and 75% consensus using in-house scripts (Suzuki et al., 2014; Tenaillon et al., 2012).

Phylogenetic tree construction

Among the strains that were sequenced, mitochondrial genomes of 12 strains were available and aligned by MAFFT (ver. 7.475) (Katoh and Standley, 2013). A phylogenetic tree was constructed using multithreaded RAxML (ver. 8.2.12) (Stamatakis, 2014), the GTRCAT model, and 1,000 bootstrap replicates, and visualized by iTOL (Letunic and Bork 2019). For chromosomal genome

phylogenetic classification, 90,987 polymorphic loci were predicted from 18 strains and concatenated, then used for construction of a phylogenetic tree by the methods described above.

Genome assembly and gene prediction

Mitochondrial genomes were assembled and annotated using GetOrganelle (ver. 1.6.4) (Jin et al., 2020) and MITOS2 (Bernt et al., 2013), respectively. To filter the mitochondrial reads, trimmed reads were aligned against mitochondrial genomes by BWA (ver. 0.7.17-r1188) (Li and Durbin, 2009), and the mapped reads were filtered by SAMtools (ver. 1.9) (Li et al., 2009) and SeqKit (Shen et al., 2016). Contigs were assembled by VelvetOptimiser (ver. 2.2.6) (Zerbino and Birney 2008), followed by generation of a simulated mate-paired library using wgsim (ver. 0.3.1-r13) (https://github.com/lh3/wgsim). The assembly of nuclear genomes was carried out by ALLPATHS-LG (ver. R52488) (Gnerre et al., 2011). The annotation of assembled nuclear genomes was performed by the Funannotate pipeline (ver. 1.7.4) (https://funannotate.readthedocs.io/en/latest/) as described previously (Takahashi et al., 2021). Following identification of repeat sequences by RepeatModeler (ver. 1.0.11) (http://www.repeatmasker.org/RepeatModeler.html) and RepeatMasker (ver. 4.0.7) (https://www.repeatmasker.org), Funannotate *ab initio* prediction was performed with the option “--busco_seed_species=aspergillus_fumigatus” by Augustus (ver. 3.3.3) (Stanke et al., 2006), GeneMark-ES (ver. 4.38) (Ter-Hovhannisyan et al., 2008), GlimmerHMM (ver. 3.0.4) (Majoros et al., 2004), and SNAP (ver. 2006-07-28) (Ian, 2004) using exon hints from the proteins of *A. fumigatus* Af293 and *N. fischeri* NRRL 181 downloaded from the *Aspergillus* Genome Database (http://www.aspgd.org/) (Cerqueira et al., 2014). The completeness of draft genomes and predicted proteins was evaluated by

BUSCO (ver. 4.0.6) (Seppey et al., 2019) with the database eurotiales_odb10. Most tools were obtained through Bioconda (Grüning et al., 2018).

Detection of orthologous genes

Orthologous relationships with *A. fumigatus* Af293 were determined by RBH with criteria BLASTp (ver. 2.9.0+) coverage >80% and identity >80% (Camacho et al., 2009).

Visualization of genome-wide distribution of SNPs and orthologous genes

SNP frequency in each 1-kb window was calculated and plotted in 250-bp steps using Python (Van Rossum and Drake 2009) and R (R Core Team 2019) scripts. The orthologous genes of *A. fumigatus* Af293 in each strain were visualized by R script.

Data availability

The genome sequencing data are deposited to DDBJ as DRA011961. BioSample accession(s): SAMD00322244-SAMD00322251.

Author contributions: HT and DH designed the research; HT, SO, YK, SU, and DH performed experiments; HT contributed new materials/tools; HT and DH analyzed data; and HT and DH wrote the manuscript.

ACKNOWLEDGMENTS

This study was supported by a grant from the Institute for Fermentation, Osaka (to DH). HT was partly supported by the National Bioscience Database Center (NBDC) of the Japan Science and Technology Agency (JST), and JSPS KAKENHI Grant Numbers 21K07001 and 16H06279. DH and HT were partly

548 supported by AMED, Grant Number JP19fm0208024. We thank Edanz
549 (https://jp.edanz.com/ac) for editing a draft of this manuscript. The authors
550 declare no competing interest.

551

552 **Figure legends**

553 **Fig. 1.** Colony growth of *Aspergillus fumigatus* strains isolated from a single tulip
554 bulb on potato-dextrose-agar (PDA) containing azoles. (A) Growth on PDA
555 containing voriconazole (VRCZ). Each strain was inoculated on PDA with
556 dimethylsulfoxide (DMSO) as a control or 10 µg/ml VRCZ, and was incubated for
557 48 h. (B) Growth on PDA containing demethylase inhibitors (DMIs). Each strain
558 was inoculated on PDA with DMSO as a control or 10 µg/ml DMI, and was
559 incubated for 48 h. (C) Colony diameter on PDA containing VRCZ or DMIs. Each
560 strain was inoculated on PDA with DMSO as a control or 10 µg/ml azole, and
561 incubated for 28 h. Error bars represent standard deviations based on three
562 independent replicates.

563

564 **Fig. 2.** Gene expression analysis by quantitative real-time (qRT)-PCR.
565 Expression levels of *cyp51A* (A) and *cdr1B* (B) were determined in the eight
566 strains isolated from a single tulip bulb. The strains were cultured in
567 potato-dextrose broth for 18 h. The *actin* gene was used as an internal control.
568 Error bars represent standard deviations based on three independent replicates.

569

570 **Fig. 3.** Microsatellite-typing analysis of *A. fumigatus* strains with tandem repeat
571 (TR) mutations. The dendrogram was constructed using short tandem repeat for
572 *A. fumigatus* (STR*Af*) patterns of the strains. The nine STR panels are shown.
573 The strains listed refer to the literature (Chen et al, 2019, Hagiwara et al, 2016b,
574 Nakano et al, 2020, Hagiwara, 2020). The names of strains isolated from plant
575 bulbs in this study or other study are highlighted in pale blue or yellow,

576 respectively. Cyp51A alleles with TR_{34} are indicated in red, and those with TR_{46}
577 in blue.
578
579 **Fig. 4.** Phylogenetic trees constructed using mitochondrial (A) and nuclear (B)
580 genomes. The trees were constructed using genomes of strains isolated from a
581 single tulip bulb (3-1-A to 3-1-H) or clinically isolated in a previous study
582 (Takahashi-Nakaguchi et al, 2016), as well as *A. fumigatus* reference strain
583 Af293.
584
585 **Fig. 5.** Differences in patterns of single nucleotide polymorphism (SNP)
586 frequency among the strains isolated from a single tulip bulb. (A) The SNP
587 presence patterns are compared in certain regions on chromosome 5 (5-A, 5-B,
588 and 5-C). (B) The patterns in each region could typically be divided into two
589 groups, which are indicated by yellow or blue panels. Ten genomic loci are
590 shown and compared among the eight strains.
591
592 **Fig. 6.** Visualization of genome-wide orthologous gene content in the strains
593 isolated from a single tulip bulb. Orthologous genes were searched against the
594 reference genome of *A. fumigatus* strain Af293. The presence of an ortholog is
595 indicated by colored ribbons for each strain (3-1-A to 3-1-H). Some regions are
596 enlarged to enable easier comparison of the patterns of gene content.
597
598 **Fig. 7.** Colony growth of *A. fumigatus* isolated from a single tulip bulb on PDA
599 containing fungicide. (A) Growth on PDA containing fungicide. Each strain was
600 inoculated onto PDA with DMSO as a control, or QoI (pyraclostrobin; 10 μg/ml),
601 SDHI (boscalid; 2.5 μg/ml), methyl benzimidazole carbamate (carbendazim; 5
602 μg/ml), or phenylpyrrole (fludioxonil; 0.2 μg/ml), and incubated for 48 h. (B)
603 Colony diameter on PDA containing fungicide. Each strain was incubated for 30

h. Error bars represent standard deviations based on three independent replicates. (C) Amino acid substitutions detected in CytB and TubA of *A. fumigatus* strains isolated from a tulip bulb.

Supporting Information

Figure S1. Genome-wide SNP frequency compared among the eight strains (3-1-A to 3-1-H). The 10 regions where the pattern is characteristically distinct among the strains are marked by red boxes.

References

Ahangarkani, F., Badali, H., Abbasi, K., Nabili, M., Khodavaisy, S., de Groot, T., and Meis, J.F. (2020) Clonal Expansion of Environmental Triazole Resistant *Aspergillus fumigatus* in Iran. *J Fungi (Basel)* **6**: 199.

Ahangarkani, F., Puts, Y., Nabili, M., Khodavaisy, S., Moazeni, M., Salehi, Z, *et al*. (2020) First azole-resistant *Aspergillus fumigatus* isolates with the environmental TR_{46} /Y121F/T289A mutation in Iran. *Mycoses* **63**: 430–436.

Saldanha, A.J. (2004) Java Treeview—extensible visualization of microarray data, *Bioinformatics* **20**: 3246–3248.

Alvarez-Moreno, C., Lavergne, R.A., Hagen, F., Morio, F., Meis, J.F., and Le Pape, P. (2017) Azole-resistant *Aspergillus fumigatus* harboring TR_{34}/L98H, TR_{46}/Y121F/T289A and TR_{53} mutations related to flower fields in Colombia. *Sci Rep* **7**: 45631.

Arora, D.S., and Kaur, N. (2019) Antimicrobial Potential of Fungal Endophytes from *Moringa oleifera*. *Appl Biochem Biotechnol* **187**: 628–648.

Bellete, B., Raberin, H., Morel, J., Flori, P., Hafid, J., and Manhsung, R.T. (2010) Acquired resistance to voriconazole and itraconazole in a patient with pulmonary aspergilloma. *Med Mycol* **48**: 197–200.

Berger, S., El Chazli, Y., Babu, A.F., and Coste, A.T. (2017) Azole Resistance in *Aspergillus fumigatus*: A Consequence of Antifungal Use in Agriculture? *Front Microbiol* **8**: 1024.

Bernt, M., Donath, A,, Jühling, F., Externbrink, F., Florentz, C., Fritzsch, G., *et al*. (2012) MITOS: improved de novo metazoan mitochondrial genome annotation. *Mol Phylogenet Evol* **69**: 313–319.

643 Bolton, M.D., Rivera, V., and Secor, G. (2013) Identification of the G143A mutation associated
644 with QoI resistance in *Cercospora beticola* field isolates from Michigan, United States. *Pest*
645 *Manag Sci* **69**: 35–39.
646
647 Buil, J.B., Hagen, F., Chowdhary, A., Verweij, P.E., and Meis, J.F. (2018) Itraconazole,
648 Voriconazole, and Posaconazole CLSI MIC Distributions for Wild-Type and Azole-Resistant
649 *Aspergillus fumigatus* Isolates. *J Fungi (Basel)* **4**: 103.
650
651 Camacho, C., Coulouris, G., Avagyan, V., Ma, N., Papadopoulos, J., Bealer, K., and Madden, T.
652 L. (2009) BLAST+: architecture and applications. *BMC Bioinformatics* **10**: 421. doi:
653 10.1186/1471-2105-10-421
654
655 Camps, S.M., Dutilh, B.E., Arendrup, M.C., Rijs, A.J., Snelders, E., Huynen, M.A., *et al*. (2012)
656 Discovery of a HapE mutation that causes azole resistance in *Aspergillus fumigatus* through
657 whole genome sequencing and sexual crossing. *PLoS One* **7**: e50034.
658
659 Cao, D., Wang, F., Yu, S., Dong, S., Wu, R., Cui, N., *et al*. (2021) Prevalence of Azole-Resistant
660 *Aspergillus fumigatus* is Highly Associated with Azole Fungicide Residues in the Fields. *Environ*
661 *Sci Technol* **55**: 3041–3049.
662
663 Cao, D., Wu, R., Dong, S., Wang, F., Ju, C., Yu, S., *et al*. (2020) Five-Year Survey (2014 to
664 2018) of Azole Resistance in Environmental *Aspergillus fumigatus* Isolates from China.
665 *Antimicrob Agents Chemother* **64**: e00904-20.
666
667 Cerqueira, G.C., Arnaud, M.B., Inglis, D.O., Skrzypek, M.S., Binkley, G., Simison, M., *et al*. (2014).
668 The Aspergillus Genome Database: multispecies curation and incorporation of RNA-Seq data to
669 improve structural gene annotations. *Nucl Acids Res* **42**: D705–D710.
670
671 Chen, Y.C., Kuo, S.F., Wang, H.C., Wu, C.J., Lin, Y.S., Li, W.S., and Lee, C.H. (2019) Azole
672 resistance in *Aspergillus* species in Southern Taiwan: An epidemiological surveillance study.
673 *Mycoses* **62**: 1174–1181.
674
675 Chen, S., Zhou, Y., Chen, Y., and Gu, J. (2018) fastp: an ultra-fast all-in-one FASTQ
676 preprocessor. *Bioinformatics* **34**: i884–i890.
677
678 Chowdhary, A., Kathuria, S., Xu, J., Sharma, C., Sundar, G., Singh, P.K., *et al*. (2012) Clonal
679 expansion and emergence of environmental multiple-triazole-resistant *Aspergillus fumigatus*
680 strains carrying the $TR_{3\,4}$/L98H mutations in the *cyp51A* gene in India. *PLoS One* **7**: e52871.
681
682 Dunne, K., Hagen, F., Pomeroy, N., Meis, J.F., and Rogers, T.R. (2017) Intercountry Transfer of
683 Triazole-Resistant *Aspergillus fumigatus* on Plant Bulbs. *Clin Infect Dis* **65**: 147–149.
684
685 Fisher, M.C., Hawkins, N.J., Sanglard, D., and Gurr, S.J. (2018) Worldwide emergence of
686 resistance to antifungal drugs challenges human health and food security. *Science* **360**:
687 739–742.
688

689 Fraaije, B., Atkins, S., Hanley, S., Macdonald, A., and Lucas, J. (2020) The Multi-Fungicide
690 Resistance Status of *Aspergillus fumigatus* Populations in Arable Soils and the Wider European
691 Environment. *Front Microbiol* **11**: 599233.
692
693 Fraczek, M.G., Bromley, M., Buied, A., Moore, C.B., Rajendran, R., Rautemaa, R., *et al*. (2013)
694 The *cdr1B* efflux transporter is associated with non-*cyp51a*-mediated itraconazole resistance in
695 *Aspergillus fumigatus*. *J Antimicrob Chemother* **68**: 1486–1496.
696
697 Francisco, J.C.E., Rivera, W.L., and Vital, P.G. (2020) Influences of carbohydrate, nitrogen, and
698 phosphorus sources on the citric acid production by fungal endophyte *Aspergillus fumigatus*
699 P3I6. *Prep Biochem Biotechnol* 50: 292–301.
700
701 Gnerre, S., Maccallum, I., Przybylski, D., Ribeiro, F.J., Burton, J.N., Walker, B.J., *et al*. (2011).
702 High-quality draft assemblies of mammalian genomes from massively parallel sequence data.
703 *Proc Natl Acad Sci U. S. A.* **108**: 1513–1518.
704
705 Grüning, B., Dale, R., Sjödin, A., Chapman, B.A., Rowe, J., Tomkins-Tinch, C. H., *et al*. (2018).
706 Bioconda: sustainable and comprehensive software distribution for the life sciences. *Nat Methods*
707 **15**: 475–476.
708
709 Hagiwara, D., Miura, D., Shimizu, K., Paul, S., Ohba, A., Gonoi, T., *et al*. (2017) A Novel
710 Zn2-Cys6 Transcription Factor AtrR Plays a Key Role in an Azole Resistance Mechanism of
711 *Aspergillus fumigatus* by Co-regulating *cyp51A* and *cdr1B* Expressions. *PLoS Pathog* **13**:
712 e1006096.
713
714 Hagiwara, D., Takahashi, H., Fujimoto, M., Sugahara, M., Misawa, Y., Gonoi, T., *et al*. (2016b)
715 Multi-azole resistant *Aspergillus fumigatus* harboring Cyp51A TR_{46}/Y121F/T289A isolated in
716 Japan. *J Infect Chemother* **22**: 577–579.
717
718 Hagiwara, D., Takahashi, H., Watanabe, A., Takahashi-Nakaguchi, A., Kawamoto, S., Kamei, K.,
719 and Gonoi, T. (2014) Whole-genome comparison of *Aspergillus fumigatus* strains serially
720 isolated from patients with aspergillosis. *J Clin Microbiol* **52**: 4202–4209.
721
722 Hagiwara, D., Watanabe, A., Kamei, K., and Goldman, G.H. (2016a) Epidemiological and
723 genomic landscape of azole resistance mechanisms in *Aspergillus* fungi. *Front Microbiol* **21**:
724 1382.
725
726 Hagiwara, D. (2020) Isolation of azole-resistant *Aspergillus fumigatus* from imported plant bulbs
727 in Japan and the effect of fungicide treatment. *J Pestic Sci* **45**: 147–150.
728
729 Hagiwara, D., Arai, T., Takahashi, H., Kusuya, Y., Watanabe, A., and Kamei, K. (2018)
730 Non-cyp51A Azole-Resistant *Aspergillus fumigatus* Isolates with Mutation in HMG-CoA
731 Reductase. *Emerg Infect Dis* **24**: 1889–1897.
732
733 Hortschansky, P., Misslinger, M., Mörl, J., Gsaller, F., Bromley, M.J., Brakhage, A.A., *et al*.
734 (2020) Structural basis of $HapE^{P88L}$-linked antifungal triazole resistance in *Aspergillus fumigatus*.
735 *Life Sci Alliance* **3**: e202000729.
736

Howard, S.J., Cerar, D., Anderson, M.J., Albarrag, A., Fisher, M.C., Pasqualotto, A.C., *et al*. (2009) Frequency and evolution of Azole resistance in *Aspergillus fumigatus* associated with treatment failure. *Emerg Infect Dis*. **15**: 1068–1076.

Ian, K. (2004). Gene finding in novel genomes. *BMC Bioinformatics* **5**: 59.

Jeanvoine, A., Rocchi, S., Bellanger, A.P., Reboux, G., and Millon, L. (2020) Azole-resistant *Aspergillus fumigatus*: A global phenomenon originating in the environment? *Med Mal Infect* **50**: 389–395.

Jenks, J.D., and Hoenigl, M. (2018) Treatment of Aspergillosis. *J Fungi (Basel)* **4**: 98.

Jin, J.J., Yu, W.B., Yang, J.B., Song, Y., de Pamphilis, C.W., Yi, T.S., et al. (2020). GetOrganelle: a fast and versatile toolkit for accurate de novo assembly of organelle genomes. *Genome Biol* **21**: 241.

Katoh, K., and Standley, D. M. (2013). MAFFT multiple sequence alignment software version 7: improvements in performance and usability. *Mol Biol Evol* **30**: 772–780.

Klaassen, C.H.W., de Valk, H.A., Balajee, S.A., and Meis, J.F.G.M. (2009) Utility of CSP typing to sub-type clinical *Aspergillus fumigatus* isolates and proposal for a new CSP type nomenclature. *J Microbiol Methods* **77**: 292–296.

Klaassen, C.H.W., Gibbons, J.G., Fedorova, N.D., Meis, J.F., and Rokas, A. (2012) Evidence for genetic differentiation and variable recombination rates among Dutch populations of the opportunistic human pathogen *Aspergillus fumigatus*. *Mol Ecol* **21:** 57–70.

Lestrade, P.P.A., Meis, J.F., Melchers, W.J.G., and Verweij, P.E. (2019) Triazole resistance in *Aspergillus fumigatus*: recent insights and challenges for patient management. *Clin Microbiol Infect* **25**: 799–806.

Letunic, I., and Bork, P. (2019). Interactive Tree Of Life (iTOL) v4: recent updates and new developments. Nucl. Acids Res. **47**, W256–W259.

Li, S., Chen, J.F., Qin, L.L., Li, X.H., Cao, Z.X., Gu, Y.C., *et al*. (2020) Two new sesquiterpenes produced by the endophytic fungus *Aspergillus fumigatus* from *Ligusticum wallichii*. *J Asian Nat Prod Res* **22**: 138–143.

Li, H., Handsaker, B., Wysoker, A., Fennell, T., Ruan, J., Homer, N., et al. (2009). The Sequence Alignment/Map format and SAMtools. *Bioinformatics* **25**: 2078–2079.

Li, H., and Durbin, R. (2009) Fast and accurate short read alignment with Burrows-Wheeler transform. *Bioinformatics* **25**: 1754–1760.

Majoros, W.H., Pertea, M., and Salzberg, S.L. (2004). TigrScan and GlimmerHMM: two open source ab initio eukaryotic gene-finders. *Bioinformatics* **20**: 2878–2879.

McKenna, A., Hanna, M., Banks, E., Sivachenko, A., Cibulskis, K., Kernytsky, A., *et al*. (2010) The Genome Analysis Toolkit: a MapReduce framework for analyzing next-generation DNA sequencing data. *Genome Res* **20**: 1297–1303.

Nakano, Y., Tashiro, M., Urano, R., Kikuchi, M., Ito, N., Moriya, E., *et al*. (2020) Characteristics of azole-resistant *Aspergillus fumigatus* attached to agricultural products imported to Japan. *J Infect Chemother* **26**: 1021–1025.

Ninomiya, A., Urayama, S.I., Suo, R., Itoi, S., Fuji, S.I., Moriyama, H., and Hagiwara, D. (2020) Mycovirus-Induced Tenuazonic Acid Production in a Rice Blast Fungus *Magnaporthe oryzae*. *Front Microbiol* **11**: 1641.

Nywening, A.V., Rybak, J.M., Rogers, P.D., and Fortwendel, J.R. (2020) Mechanisms of triazole resistance in *Aspergillus fumigatus*. *Environ Microbiol* **22**: 4934–4952.

O'Gorman, C.M., Fuller, H.T., and Dyer, P.S. (2009) Discovery of a sexual cycle in the opportunistic fungal pathogen *Aspergillus fumigatus*. *Nature* **457:** 471–474.

Pontes, L., Beraquet, C.A.G., Arai, T., Pigolli, G.L., Lyra, L., Watanabe, A., *et al*. (2020) *Aspergillus fumigatus* Clinical Isolates Carrying CYP51A with TR_{34}/L98H/S297T/F495I Substitutions Detected after Four-Year Retrospective Azole Resistance Screening in Brazil. *Antimicrob Agents Chemother* **64**: e02059-19.

Price, C.L., Parker, J.E., Warrilow, A.G., Kelly, D.E., and Kelly, S.L. (2015) Azole fungicides - understanding resistance mechanisms in agricultural fungal pathogens. *Pest Manag Sci* **71**: 1054–1058.

Qin, W., Liu, C., Jiang, W., Xue, Y., Wang, G., and Liu, S. (20190 A coumarin analogue NFA from endophytic *Aspergillus fumigatus* improves drought resistance in rice as an antioxidant. *BMC Microbiol* **19**: 50.

R Core Team (2019). R: A language and environment for statistical computing. R Foundation for Statistical Computing, Vienna, Austria. URL https://www.R-project.org/.

Resendiz Sharpe, A., Lagrou, K., Meis, J.F., Chowdhary, A., Lockhart, S.R., and Verweij, P.E. (2018) ISHAM/ECMM Aspergillus Resistance Surveillance working group. Triazole resistance surveillance in *Aspergillus fumigatus*. *Med Mycol* **56**(suppl_1): 83–92.

Rybak, J.M., Ge, W., Wiederhold, N.P., Parker, J.E., Kelly, S.L., Rogers, P.D., and Fortwendel, J.R. (2019) Mutations in *hmg1*, Challenging the Paradigm of Clinical Triazole Resistance in *Aspergillus fumigatus*. *mBio* **10**: e00437-19.

Samuel, S., Papayiannis, L.C., Leroch, M., Veloukas, T., Hahn, M., and Karaoglanidis, G.S. (2011) Evaluation of the incidence of the G143A mutation and *cytb* intron presence in the cytochrome bc-1 gene conferring QoI resistance in *Botrytis cinerea* populations from several hosts. *Pest Manag Sci* **67**: 1029–1036.

Schoustra, S.E., Debets, A.J.M., Rijs, A.J.M.M., Zhang, J., Snelders, E., Leendertse, P.C., *et al*. (2019) Environmental Hotspots for Azole Resistance Selection of *Aspergillus fumigatus*, the Netherlands. *Emerg Infect Dis* **25**: 1347–1353.

Seppey, M., Manni, M., and Zdobnov, E.M. (2019). BUSCO: assessing genome assembly and annotation completeness. *Methods Mol Biol* **1962**: 227–245.

Sewell, T.R., Zhu, J., Rhodes, J., Hagen, F., Meis, J.F., Fisher, M.C., and Jombart, T. (2019) Nonrandom Distribution of Azole Resistance across the Global Population of *Aspergillus fumigatus*. *mBio* **10**: e00392-19.

Shen, W., Le, S., Li, Y., and Hu, F. (2016). SeqKit: A cross-platform and ultrafast toolkit for FASTA/Q file manipulation. *PLoS ONE* **11**: e0163962.

Snelders, E., Camps, S.M., Karawajczyk, A., Schaftenaar, G., Kema, G.H., van der Lee, H.A., *et al*. (2012) Triazole fungicides can induce cross-resistance to medical triazoles in *Aspergillus fumigatus*. *PLoS One* **7**: e31801.

Stamatakis, A. (2014). RAxML version 8: a tool for phylogenetic analysis and post-analysis of large phylogenies. *Bioinformatics* **30**: 1312–1313.

Stanke, M., Schöffmann, O., Morgenstern, B., and Waack, S. (2006) Gene prediction in eukaryotes with a generalized hidden Markov model that uses hints from external sources. *BMC Bioinformatics* **7**: 62.

Suzuki, S., Horinouchi, T., and Furusawa, C. (2014) Prediction of antibiotic resistance by gene expression profiles. *Nat Commun* **5**: 5792.

Takahashi-Nakaguchi, A., Muraosa, Y., Hagiwara, D., Sakai, K., Toyotome, T., Watanabe, A., *et al*. (2015) Genome sequence comparison of *Aspergillus fumigatus* strains isolated from patients with pulmonary aspergilloma and chronic necrotizing pulmonary aspergillosis. *Med Mycol* **53**: 353–360.

Takahashi, H., Umemura, M., Ninomiya, A., Kusuya, Y., Shimizu, M., Urayama, S., *et al*. (2021) Interspecies Genomic Variation and Transcriptional Activeness of Secondary Metabolism-Related Genes in Aspergillus Section Fumigati. *Front Fungal Biol* **2**: 656751. doi: 10.3389/ffunb.2021.656751

Tenaillon, O., Rodríguez-Verdugo, A., Gaut, R.L., McDonald, P., Bennett, A.F., Long, A.D., *et al*. (2012) The molecular diversity of adaptive convergence. *Science* **335**: 457–461.

Ter-Hovhannisyan, V., Lomsadze, A., Chernoff, Y. O., and Borodovsky, M. (2008) Gene prediction in novel fungal genomes using an ab initio algorithm with unsupervised training. *Genome Res* **18**: 1979–1990.

Toyotome, T., Fujiwara, T., Kida, H., Matsumoto, M., Wada, T., and Komatsu, R. (2016) Azole susceptibility in clinical and environmental isolates of *Aspergillus fumigatus* from eastern Hokkaido, Japan. *J Infect Chemother* 22: 648–650.

Wang, H.C., Huang, J.C., Lin, Y.H., Chen, Y.H., Hsieh, M.I., Choi, P.C., *et al*. (2018) Prevalence, mechanisms and genetic relatedness of the human pathogenic fungus *Aspergillus fumigatus* exhibiting resistance to medical azoles in the environment of Taiwan. *Environ Microbiol* **20**: 270–280.

Yarden, O., and Katan, T. (1993). Mutations leading to substitutions at amino acid 198 and 200 of beta–tubulin that correlate with benomyl-resistant phenotypes of field strains of *Botrytis cinerea. Phytopathology* **83**: 1478–1483.

Zerbino, D.R., and Birney, E. (2008) Velvet: algorithms for de novo short read assembly using de Bruijn graphs. *Genome Res* **18**: 821–829.

Zhang, J., Lopez Jimenez, L., Snelders, E., Debets, A.J.M., Rietveld, A.G., Zwaan, B.J., *et al*. (2021) Dynamics of *Aspergillus fumigatus* in Azole Fungicide-Containing Plant Waste in the Netherlands (2016-2017). *Appl Environ Microbiol* **87**: e02295-20.

Zhang, J., Snelders, E., Zwaan, B.J., Schoustra, S.E., Meis, J.F., van Dijk, K., *et al*. (2017) A Novel Environmental Azole Resistance Mutation in *Aspergillus fumigatus* and a Possible Role of Sexual Reproduction in Its Emergence. *mBio* **8**: e00791-17.

Zhou, D., Korfanty, G.A., Mo, M., Wang, R., Li, X., Li, H., *et al*. (2021) Extensive Genetic Diversity and Widespread Azole Resistance in Greenhouse Populations of *Aspergillus fumigatus* in Yunnan, China. *mSphere* **6**: e00066-21.

Zhou, Z., Duan, Y., and Zhou, M. (2020) Carbendazim-resistance associated β_2 -tubulin substitutions increase deoxynivalenol biosynthesis by reducing the interaction between β_2 -tubulin and IDH3 in *Fusarium graminearum*. *Environ Microbiol* **22**: 598–614.

de Hoon, M.J., Imoto, S., Nolan, J., and Miyano, S. (2004) Open source clustering software. *Bioinformatics* **20**: 1453–1454.

de Valk, H.A., Meis, J.F., Curfs, I.M., Muehlethaler, K., Mouton, J.W., and Klaassen, C.H. (2005) Use of a novel panel of nine short tandem repeats for exact and high-resolution fingerprinting of *Aspergillus fumigatus* isolates. *J Clin Microbiol* **43**: 4112–4120.

van Ingen, J., van der Lee, H.A., Rijs, T.A., Zoll, J., Leenstra, T., Melchers, W.J., and Verweij, P.E. (2015) Azole, polyene and echinocandin MIC distributions for wild-type, TR_{34}/L98H and TR46/Y121F/T289A *Aspergillus fumigatus* isolates in the Netherlands. *J Antimicrob Chemother* **70**: 178–181.

Van Rossum, G., and Drake, F. L. (2009) Python 3 Reference Manual. Scotts Valley, CA: CreateSpace.

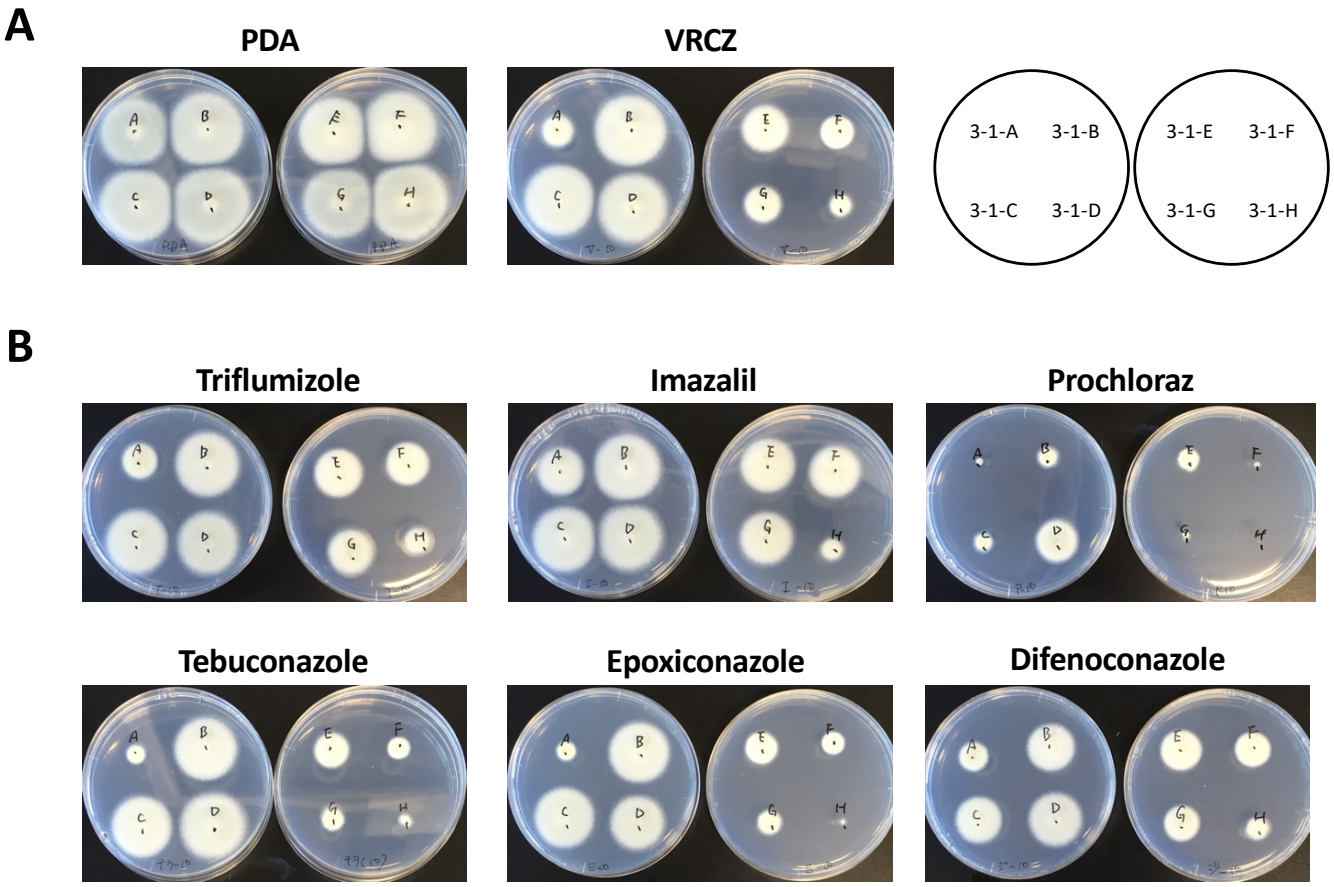

Fig. 1

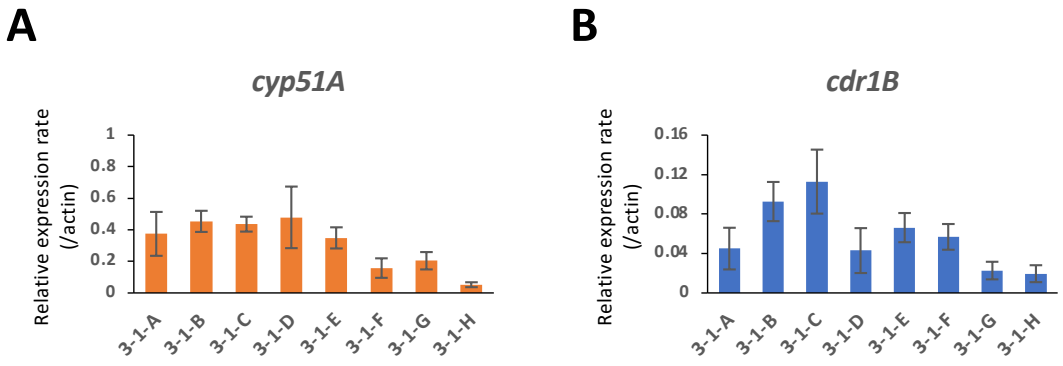

Fig. 2

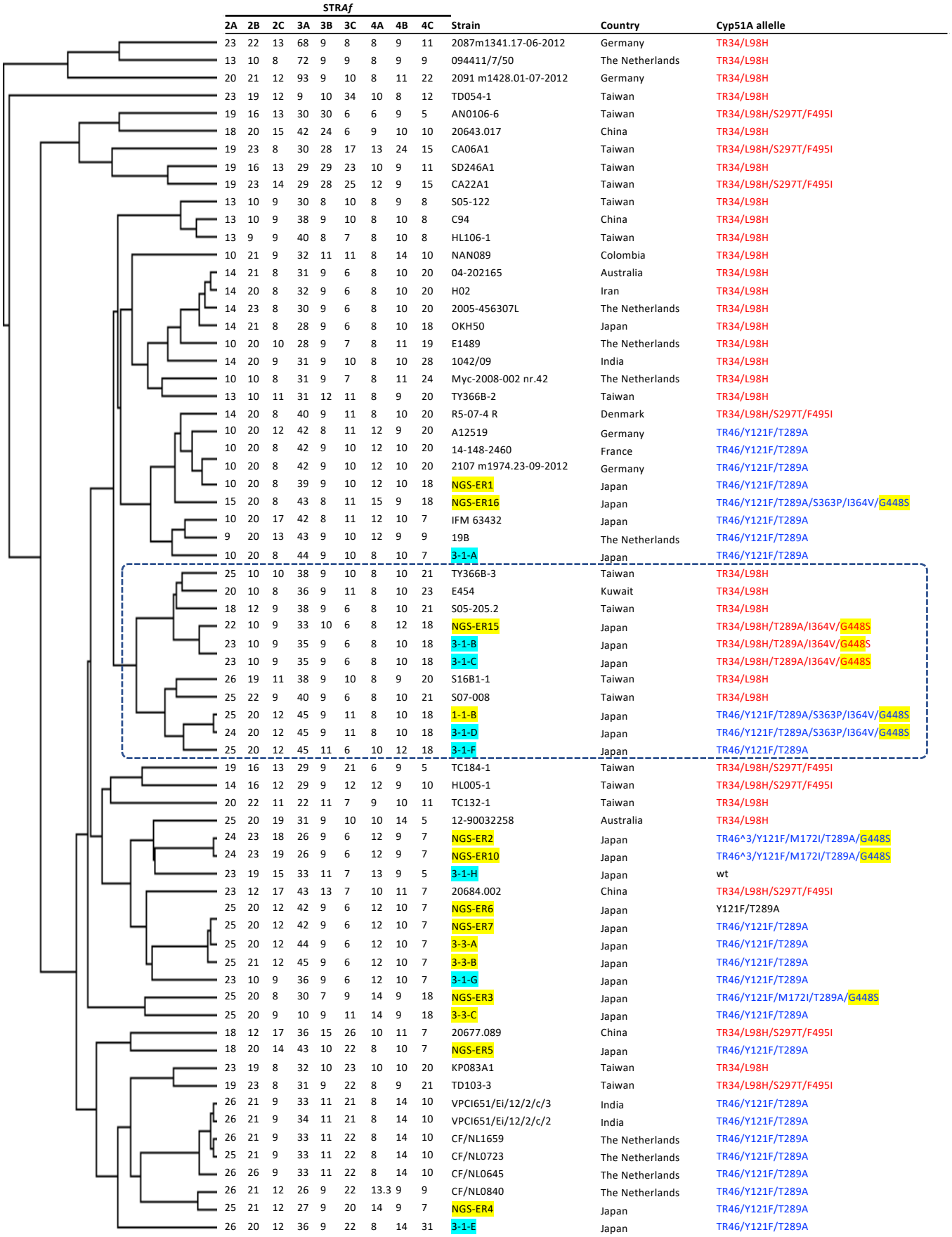

STR*Af*											
2A	2B	2C	3A	3B	3C	4A	4B	4C	Strain	Country	Cyp51A allele
23	22	13	68	9	8	8	9	11	2087m1341.17-06-2012	Germany	TR34/L98H
13	10	8	72	9	9	8	9	9	094411/7/50	The Netherlands	TR34/L98H
20	21	12	93	9	10	8	11	22	2091 m1428.01-07-2012	Germany	TR34/L98H
23	19	12	9	10	34	10	8	12	TD054-1	Taiwan	TR34/L98H
19	16	13	30	30	6	6	9	5	AN0106-6	Taiwan	TR34/L98H/S297T/F495I
18	20	15	42	24	6	9	10	10	20643.017	China	TR34/L98H
19	23	8	30	28	17	13	24	15	CA06A1	Taiwan	TR34/L98H/S297T/F495I
19	16	13	29	29	23	10	9	11	SD246A1	Taiwan	TR34/L98H
19	23	14	29	28	25	12	9	15	CA22A1	Taiwan	TR34/L98H/S297T/F495I
13	10	9	30	8	10	8	9	8	S05-122	Taiwan	TR34/L98H
13	10	9	38	9	10	8	10	8	C94	China	TR34/L98H
13	9	9	40	8	7	8	10	8	HL106-1	Taiwan	TR34/L98H
10	21	9	32	11	11	8	14	10	NAN089	Colombia	TR34/L98H
14	21	8	31	9	6	8	10	20	04-202165	Australia	TR34/L98H
14	20	8	32	9	6	8	10	20	H02	Iran	TR34/L98H
14	23	8	30	9	6	8	10	20	2005-456307L	The Netherlands	TR34/L98H
14	21	8	28	9	6	8	10	18	OKH50	Japan	TR34/L98H
10	20	10	28	9	7	8	11	19	E1489	The Netherlands	TR34/L98H
14	20	9	31	9	10	8	10	28	1042/09	India	TR34/L98H
10	10	8	31	9	7	8	11	24	Myc-2008-002 nr.42	The Netherlands	TR34/L98H
13	10	11	31	12	11	8	9	20	TY366B-2	Taiwan	TR34/L98H
14	20	8	40	9	11	8	10	20	R5-07-4 R	Denmark	TR34/L98H/S297T/F495I
10	20	12	42	8	11	12	9	20	A12519	Germany	TR46/Y121F/T289A
10	20	8	42	9	10	12	10	20	14-148-2460	France	TR46/Y121F/T289A
10	20	8	42	9	10	12	10	20	2107 m1974.23-09-2012	Germany	TR46/Y121F/T289A
10	20	8	39	9	10	12	10	18	NGS-ER1	Japan	TR46/Y121F/T289A
15	20	8	43	8	11	15	9	18	NGS-ER16	Japan	TR46/Y121F/T289A/S363P/I364V/G448S
10	20	17	42	8	11	12	10	7	IFM 63432	Japan	TR46/Y121F/T289A
9	20	13	43	9	10	12	9	9	19B	The Netherlands	TR46/Y121F/T289A
10	20	8	44	9	10	8	10	7	3-1-A	Japan	TR46/Y121F/T289A
25	10	10	38	9	10	8	10	21	TY366B-3	Taiwan	TR34/L98H
20	10	8	36	9	11	8	10	23	E454	Kuwait	TR34/L98H
18	12	9	38	9	6	8	10	21	S05-205.2	Taiwan	TR34/L98H
22	10	9	33	10	6	8	12	18	NGS-ER15	Japan	TR34/L98H/T289A/I364V/G448S
23	10	9	35	9	6	8	10	18	3-1-B	Japan	TR34/L98H/T289A/I364V/G448S
23	10	9	35	9	6	8	10	18	3-1-C	Japan	TR34/L98H/T289A/I364V/G448S
26	19	11	38	9	10	8	9	20	S16B1-1	Taiwan	TR34/L98H
25	22	9	40	9	6	8	10	21	S07-008	Taiwan	TR34/L98H
25	20	12	45	9	11	8	10	18	1-1-B	Japan	TR46/Y121F/T289A/S363P/I364V/G448S
24	20	12	45	9	11	8	10	18	3-1-D	Japan	TR46/Y121F/T289A/S363P/I364V/G448S
25	20	12	45	11	6	10	12	18	3-1-F	Japan	TR46/Y121F/T289A
19	16	13	29	9	21	6	9	5	TC184-1	Taiwan	TR34/L98H/S297T/F495I
14	16	12	29	9	12	12	9	10	HL005-1	Taiwan	TR34/L98H/S297T/F495I
20	22	11	22	11	7	9	10	11	TC132-1	Taiwan	TR34/L98H
25	20	19	31	9	10	10	14	5	12-90032258	Australia	TR34/L98H
24	23	18	26	9	6	12	9	7	NGS-ER2	Japan	TR46^3/Y121F/M172I/T289A/G448S
24	23	19	26	9	6	12	9	7	NGS-ER10	Japan	TR46^3/Y121F/M172I/T289A/G448S
23	19	15	33	11	7	13	9	5	3-1-H	Japan	wt
23	12	17	43	13	7	10	11	7	20684.002	China	TR34/L98H/S297T/F495I
25	20	12	42	9	6	12	10	7	NGS-ER6	Japan	Y121F/T289A
25	20	12	42	9	6	12	10	7	NGS-ER7	Japan	TR46/Y121F/T289A
25	20	12	44	9	6	12	10	7	3-3-A	Japan	TR46/Y121F/T289A
25	21	12	45	9	6	12	10	7	3-3-B	Japan	TR46/Y121F/T289A
23	10	9	36	9	6	12	10	7	3-1-G	Japan	TR46/Y121F/T289A
25	20	8	30	7	9	14	9	18	NGS-ER3	Japan	TR46/Y121F/M172I/T289A/G448S
25	20	9	10	9	11	14	9	18	3-3-C	Japan	TR46/Y121F/T289A
18	12	17	36	15	26	10	11	7	20677.089	China	TR34/L98H/S297T/F495I
18	20	14	43	10	22	8	10	7	NGS-ER5	Japan	TR46/Y121F/T289A
23	19	8	32	10	23	10	10	20	KP083A1	Taiwan	TR34/L98H
19	23	8	31	9	22	8	9	21	TD103-3	Taiwan	TR34/L98H/S297T/F495I
26	21	9	33	11	21	8	14	10	VPCI651/Ei/12/2/c/3	India	TR46/Y121F/T289A
26	21	9	34	11	21	8	14	10	VPCI651/Ei/12/2/c/2	India	TR46/Y121F/T289A
26	21	9	33	11	22	8	14	10	CF/NL1659	The Netherlands	TR46/Y121F/T289A
25	21	9	33	11	22	8	14	10	CF/NL0723	The Netherlands	TR46/Y121F/T289A
26	26	9	33	11	22	8	14	10	CF/NL0645	The Netherlands	TR46/Y121F/T289A
26	21	12	26	9	22	13.3	9	9	CF/NL0840	The Netherlands	TR46/Y121F/T289A
25	21	12	27	9	20	14	9	7	NGS-ER4	Japan	TR46/Y121F/T289A
26	20	12	36	9	22	8	14	31	3-1-E	Japan	TR46/Y121F/T289A

Fig. 3

A

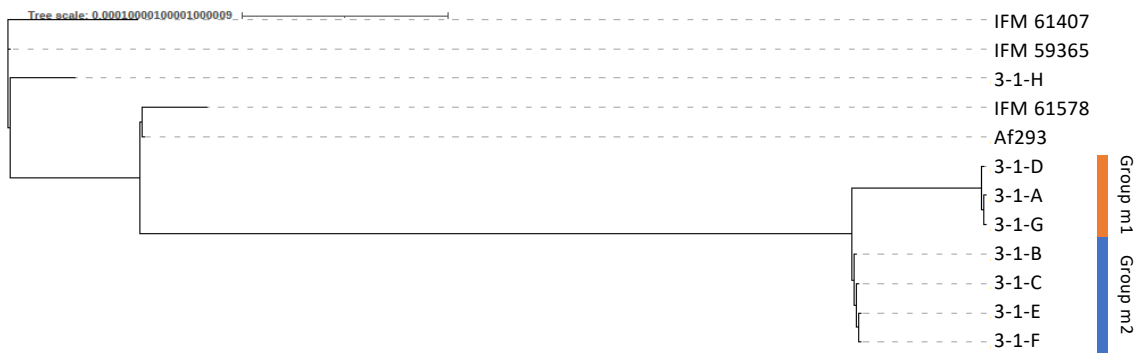
Tree scale: 0.0001000010000100000 9
IFM 61407
IFM 59365
3-1-H
IFM 61578
Af293
3-1-D
3-1-A
3-1-G
3-1-B
3-1-C
3-1-E
3-1-F
Group m1
Group m2

B

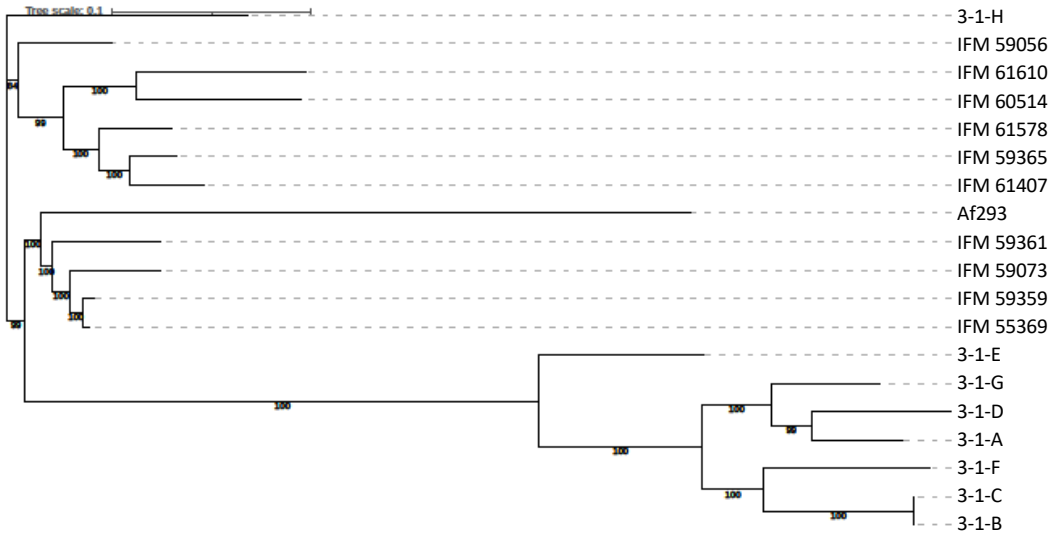
Tree scale: 0.1
3-1-H
IFM 59056
IFM 61610
IFM 60514
IFM 61578
IFM 59365
IFM 61407
Af293
IFM 59361
IFM 59073
IFM 59359
IFM 55369
3-1-E
3-1-G
3-1-D
3-1-A
3-1-F
3-1-C
3-1-B

Fig. 4

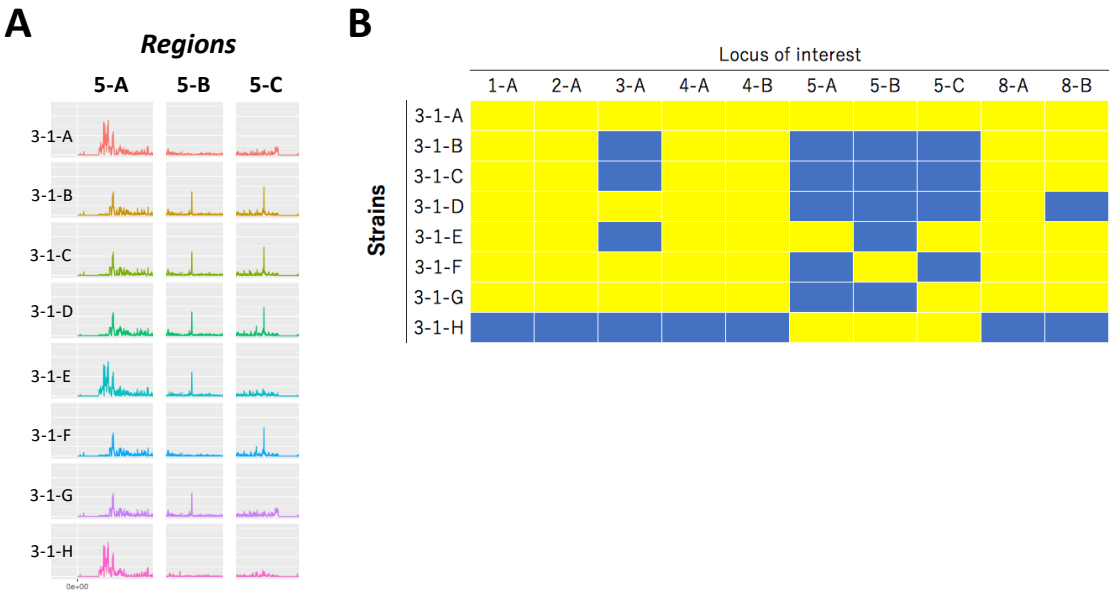
A
Regions
5-A
5-B
5-C
3-1-A
3-1-B
3-1-C
3-1-D
3-1-E
3-1-F
3-1-G
3-1-H
0e+00
B
Locus of interest
1-A
2-A
3-A
4-A
4-B
5-A
5-B
5-C
8-A
8-B
Strains
3-1-A
3-1-B
3-1-C
3-1-D
3-1-E
3-1-F
3-1-G
3-1-H

Fig. 5

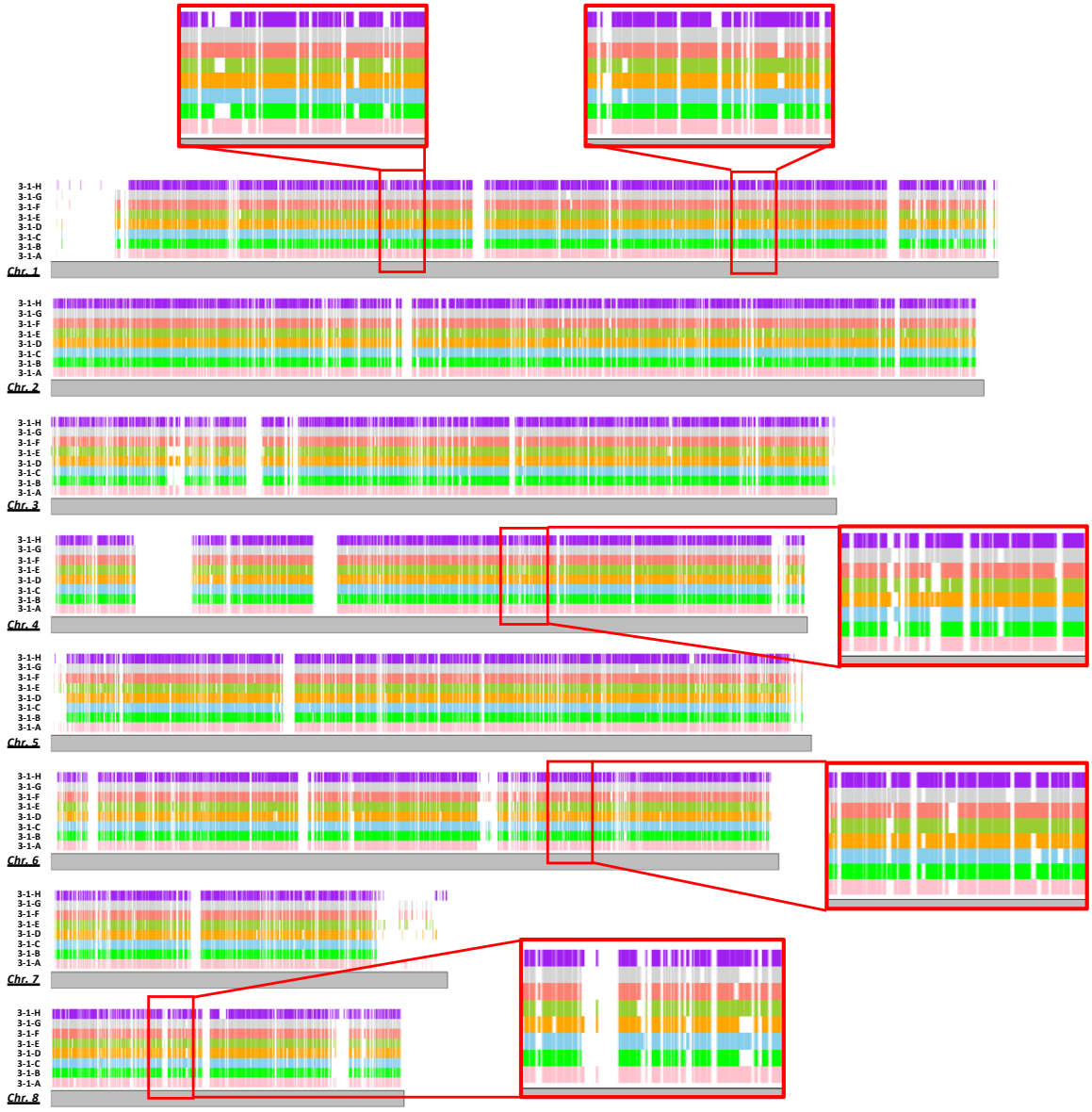
3-1-H
3-1-G
3-1-F
3-1-E
3-1-D
3-1-C
3-1-B
3-1-A
Chr. 1
Chr. 2
Chr. 3
Chr. 4
Chr. 5
Chr. 6
Chr. 7
Chr. 8

Fig. 6

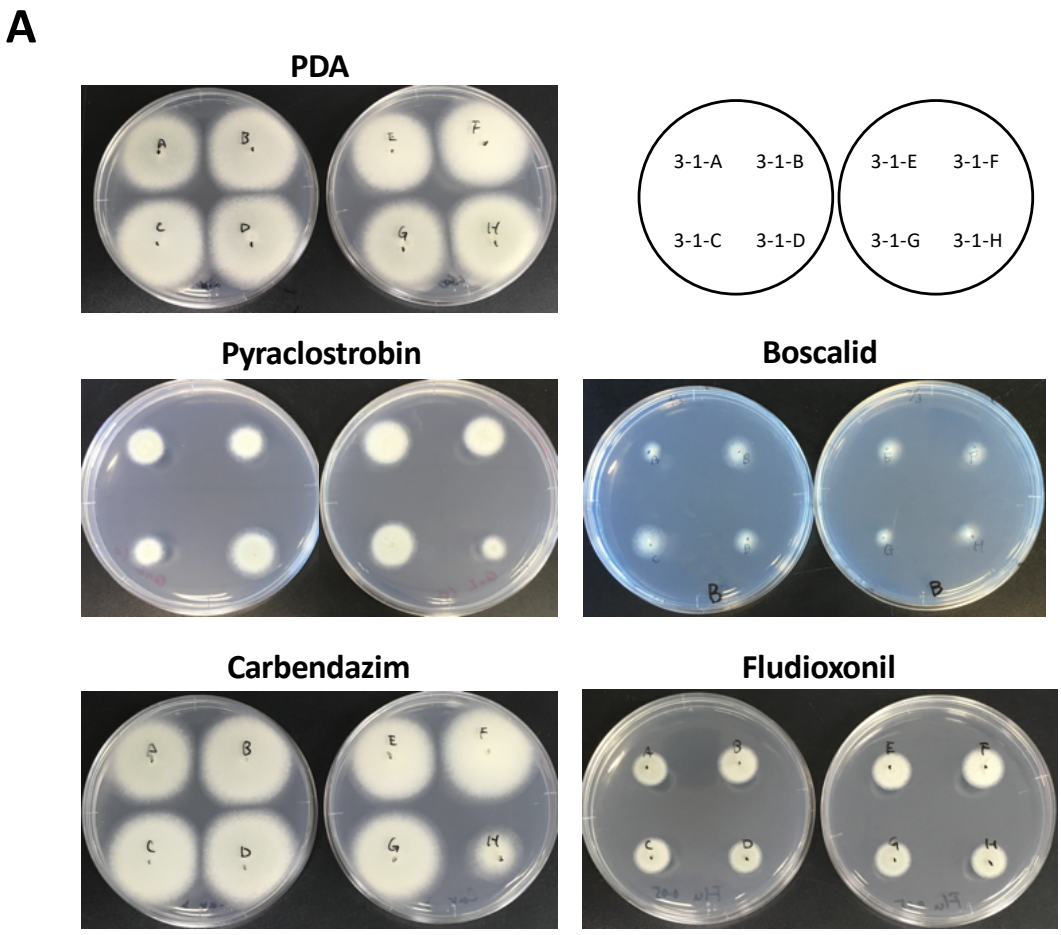
A
PDA
3-1-A
3-1-B
3-1-C
3-1-D
3-1-E
3-1-F
3-1-G
3-1-H
Pyraclostrobin
Boscalid
Carbendazim
Fludioxonil
B
Colony diameter [mm]
30
20
10
0
PDA
Pyraclostrobin
Carbendazim
Boscalid
Fludioxonil
C
CytB (385 aa)
TubA (466 aa)
V131 (3-1-A to 3-1-G)
V119I (3-1-H)
G143A (3-1-A to 3-1-G)
F219Y (3-1-A to 3-1-G)

Fig. 7